

Fault creep and microseismicity on the Hayward fault, California: Implications for asperity size

Christine R. Gans and Kevin P. Furlong

Geodynamics Research Group, Department of Geosciences, Pennsylvania State University, University Park, Pennsylvania, USA

Rocco Malservisi

Rosenstiel School of Marine and Atmospheric Science, University of Miami, Miami, Florida, USA

Received 5 June 2003; revised 26 August 2003; accepted 3 September 2003; published 10 October 2003.

[1] The Hayward fault is documented to undergo significant creep, with some patches accommodating 50% or more of the long-term fault displacement. In spite of this, the fault has also experienced moderate to large earthquakes. By comparing the patterns of microseismicity observed on the fault with models of fault zone creep, we can investigate the long-term displacement/deformation history of the fault in terms of the relative roles of aseismic creep, fault slip accommodated through microseismicity, and strain accumulation (slip deficit). We find that microseismicity on the Hayward fault produces a negligible percentage of the seismic moment dissipated on the fault. Combining seismicity with our fault creep models allows us to calculate the size of asperities on the creeping fault. For small asperities associated with repeating earthquakes on the Hayward fault, the rupture areas of these asperities range from 20 to 60 m².

INDEX TERMS: 7209 Seismology: Earthquake dynamics and mechanics; 7215 Seismology: Earthquake parameters; 7223 Seismology: Seismic hazard assessment and prediction; 7230 Seismology: Seismicity and seismotectonics. **Citation:** Gans, C. R., K. P. Furlong, and R. Malservisi, Fault creep and microseismicity on the Hayward fault, California: Implications for asperity size, *Geophys. Res. Lett.*, 30(19), 2000, doi:10.1029/2003GL017904, 2003.

1. Introduction

[2] The Hayward fault, located on the east side of the San Francisco Bay, California (Figure 1), is one of a limited set of faults documented to undergo creep [e.g., *Lienkaemper et al.*, 1991; *Galehouse*, 1992; *Lienkaemper and Galehouse*, 1998]. Creeping segments of strike-slip faults are often characterized by high rates of microseismicity on or near the fault [*Scholz*, 1990; *Rubin et al.*, 1999; *Amelung and King*, 1997; *Waldhauser and Ellsworth*, 2002]. It is normally assumed that this microseismicity generates only a small fraction of the slip occurring on the fault and that a majority of the accumulating elastic strain is released either through aseismic creep or in rare large events. Models of fault creep allow us to test this assumption. We compare over a ten year period the inferred slip of microearthquakes determined from magnitude/energy relationships with slip modeled for aseismic creep to quantify the role of microseismicity on a creeping fault.

[3] In previous work [*Malservisi et al.*, 2003; *Malservisi*, 2002], we used 3-D finite element modeling to investigate creep patterns on the Hayward fault. When developing our models of creep, we did not explicitly model any earthquakes (cf. *Bürgmann et al.* [2000]; *Simpson et al.* [2001]); rather we assumed that all displacements that occurred on the fault during the inter-seismic period between large earthquakes were accommodated by aseismic creep. Although it is typically assumed that microseismicity accounts for a negligible proportion of the moment released on creeping faults, to our knowledge this assumption has not been tested. Because creeping faults are characterized by relatively high levels of microseismicity, it is important to understand what role, if any, the seismicity plays in fault displacements.

[4] Our modeled estimate of aseismic slip can also be combined with moments for repeating earthquakes in the creeping zones to infer the size of the rupture areas for the small asperities associated with these earthquakes. There is considerable debate on the actual dimensions of these locked patches on a fault plane [e.g., *Aki*, 1967; *Archuleta et al.*, 1982; *Aki*, 1987; *Abercrombie*, 1995; *Nadeau and Johnson*, 1998]. Here we develop an approach for constraining the size of small asperities by combining our model of creep on the Hayward fault with event characteristics from the precise relative relocations of micro-earthquakes [*Waldhauser and Ellsworth*, 2002]. Typically in order to calculate asperity size, the amount of slip associated with the rupture of a locked patch is assumed. By exploiting models of creep on fault planes [e.g., *Bürgmann et al.*, 2000; *Simpson et al.*, 2001; *Malservisi*, 2002; *Malservisi et al.*, 2003], however, we have an independent estimate of that slip. Thus we use a direct estimate for slip in the vicinity of the asperity [*Malservisi*, 2002; *Malservisi et al.*, 2003], which is independent of earthquake size/slip laws. This reduces some of the circularity in the asperity size analysis. This approach for determining asperity sizes and their distribution on the fault plane allows us to place constraints on the geologic characteristics of an asperity.

2. Calculating Slip for Micro-Earthquakes

[5] Patterns of microseismicity are well documented on the Hayward fault. However, whether this microseismicity plays any significant role in the observed fault creep is not known. For example, although near-surface creep appears to be virtually aseismic, it is not clear whether the inter-seismic slip (creep) occurring at depth is also fully aseismic.

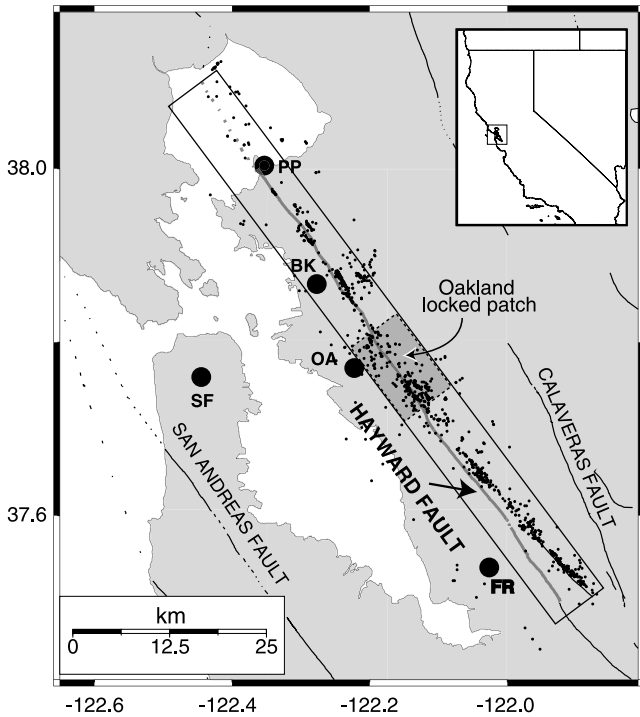


Figure 1. San Francisco Bay area map with Hayward fault seismicity. The map shows the location of the geographical references used in the text and the main faults of the San Andreas fault system in the region [Jennings, 1994]. The relocated seismicity from Waldhauser and Ellsworth [2002] is indicated by the small solid dots. The Hayward fault and vicinity are outlined by the box, with the surface trace of the fault marked by the thicker gray line. (PP-Point Pinole, BK-Berkeley, OA-Oakland, FR-Fremont, SF-San Francisco)

[6] We have used precise relative relocations of micro-earthquakes spanning 1984 to 1998 [Waldhauser and Ellsworth, 2002]. A total of 976 earthquakes, with magnitudes ranging from $M_1 = \sim 0.5$ to 4.5, on average 1 to 2, and located within 2 km of the fault plane were chosen from the set of 1251 (Figure 2). Of these, 250 were identified as repeating by Waldhauser and Ellsworth [2002]. Because of their nearly identical waveforms and common locations, these events identified as repeating likely represent the repeated rupture of the same patch or asperity on the fault plane.

[7] To determine the amount of slip that occurred with each micro-earthquake, we used scaling relationships for earthquakes to estimate displacement from local magni-

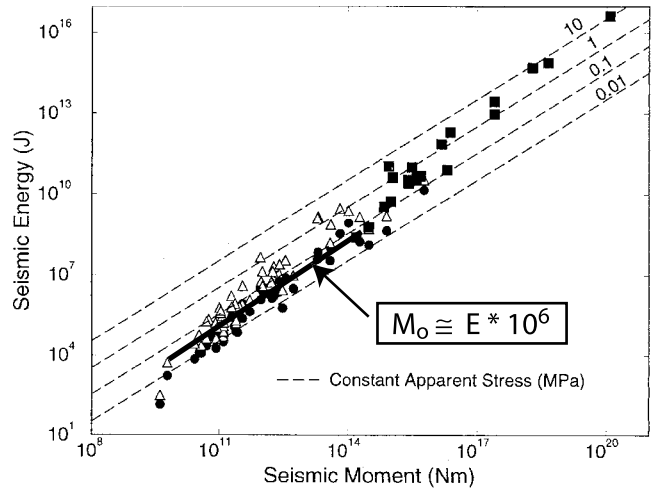


Figure 3. Seismic Energy (J) versus Seismic Moment (N·m) from Abercrombie [1995]. Solid line is our “best-fit” through the data in the energy range of the Hayward microseismicity dataset.

tude. We combine magnitude/energy, energy/moment and moment/displacement relationships to do this. Several relations for calculating energy from magnitude are available [e.g., Smith and Wyss, 1968; Bath, 1978; Kanamori et al., 1993]. We have used the Thatcher and Hanks [1973] relation, which was developed for earthquakes in southern California:

$$\text{Log}(E) = 2.0 M_1 + 8.1 \quad (1)$$

where E is the energy in ergs and M_1 is the local magnitude. It should be noted, however, that this relation is optimally used for earthquakes with magnitudes greater than 3.5, and only $\sim 1\%$ of our earthquakes are $M_1 > 3.5$.

[8] To move from energy to moment, we have used the relationship from Abercrombie [1995] for calculating the seismic moment. For this study the moment magnitude to energy relationship $M_o = E * 10^6$ was used (Figure 3), where M_o is the seismic moment in N·m and E is the energy in J. We assume a constant stress drop of ~ 0.8 MPa, based on our best-fit from Abercrombie’s [1995] data. Our choice of magnitude/energy relationship has only a small effect on our results. For example, if we compare the total moment from the seismicity obtained using the Thatcher and Hanks [1973] model (1.6×10^{10} N·m) with that using the Kanamori et al. [1993] model (9.6×10^{10} N·m), we find a factor of 6 difference in the results. As we show below,

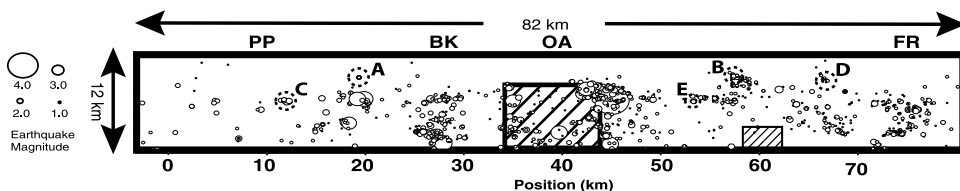


Figure 2. Fault-plane view of the Hayward fault, Model KT3 from Malservisi [2002] (see Figure 1 for location). Precisely-relocated micro-earthquakes from Waldhauser and Ellsworth [2002] are shown by circles scaled by magnitude. A through E mark several potential asperity locations (see text for details). Letters (PP, BK, OA, FR) correspond to locations from Figure 1.

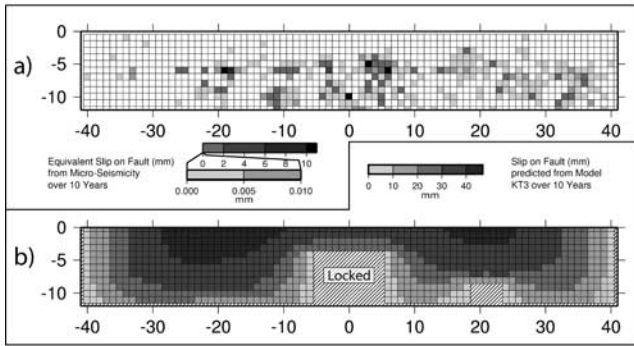


Figure 4. Slip (in mm) accumulated on the Hayward fault over 10 years. (a) Equivalent slip attributable to microseismicity. (b) Slip predicted from our model (KT3). Note the different scales between (a) and (b).

this difference is insignificant when compared to the moment released through creep.

[9] The slip from each earthquake was calculated using

$$D = Mo / (\mu * A) \quad (2)$$

where D is the slip on the fault in meters during the earthquake, Mo is the seismic moment in N-m, A is the source area in m^2 , and μ is the shear modulus (assumed to be ~ 30 GPa). To compare the slip dissipated by micro-earthquakes to the slip from creep, we scale the slip from the microseismicity to 1 km^2 areas, the element size for our creep models. We sum the seismic moments (Mo) for earthquakes within each 1 km^2 element and divide by its area (A) to determine the equivalent slip (D) in a given element.

2.1. Partitioning Between Creep and Microseismicity

[10] We compare the slip generated by micro-earthquakes within each element with the creep inferred from model KT3 [Figure 4, *Malservisi*, 2002] to assess the relative contributions of seismic and aseismic slip. Figure 4 shows the equivalent slip (per 1 km^2) on the Hayward fault from both microseismicity and fault creep from our model, over a ten-year period. Note the significantly different scales for slip magnitude between the microseismicity and creep plots. For microseismicity, almost all elements have less than 0.005 mm slip over the ten year period, whereas the contribution from creep can range up to 45 mm . Averaged over the entire fault plane, the slip from the microseismicity is $5.4 \times 10^{-7} \text{ mm/yr}$, whereas the slip from creep averages 2.4 mm/yr over the fault plane. Using the relationships of *Smith and Wyss* [1968], *Båth* [1978] or *Kanamori et al.* [1993] that maximize the slip from seismicity, the average slip from microseismicity becomes 2.2×10^{-5} , 8.5×10^{-6} and $3.3 \times 10^{-6} \text{ mm/yr}$, respectively. Thus microseismic slip remains insignificant when compared to the slip contribution due to creep. The occasional element with a larger seismic slip value (maximum 5.6 mm/yr) comes from the rare, larger magnitude ($M_1 \sim 4-4.5$) earthquakes on the Hayward fault.

[11] Along the entire 82 km length of the fault studied, various numerical models of creep generate similar values of moment accumulation per year: Model KT3 (this paper) produces $1.98 \times 10^{17} \text{ N}\cdot\text{m/yr}$, the model of *Bürgmann et al.*

[2000] produces $1.92 \times 10^{17} \text{ N}\cdot\text{m/yr}$, and the *Simpson et al.* [2001] model accumulates $2.01 \times 10^{17} \text{ N}\cdot\text{m/yr}$. If no creep occurred on the fault (it remained locked throughout), the seismic moment would accumulate at a rate of $2.7 \times 10^{17} \text{ N}\cdot\text{m/yr}$. In other words, creep releases approximately 25% of the potential moment accumulation rate on the fault.

[12] Aseismic creep dissipates virtually all of the moment that is expended during intervals between large ($M_1 > 6$) earthquakes. This reinforces the assumption that micro-earthquakes are not important contributors to the total strain released on a fault, and here we can quantify ($< 0.01\%$ of the total interseismic slip) this small contribution. Further, although the numerical creep models of *Malservisi et al.* [2003], *Malservisi* [2002], and those from other groups (*Bürgmann et al.* [2000]; *Simpson et al.* [2001]) did not include slip from seismicity, our results suggest that these models can be viewed as accurate portraits of creep on the fault plane.

3. Asperity Size

[13] Using our creep models to constrain the amount of slip for specific micro-earthquakes, we can estimate the size of an asperity on a fault plane. The asperities we focus on are patches on the fault that are inferred to fail repeatedly as they are loaded by creep on the surrounding fault surface [*Waldhauser and Ellsworth*, 2002]. The geometry and dimensions of such asperities are poorly constrained, and characteristic minimum source dimensions have previously been argued to range from less than 1 cm [*Johnson and Nadeau*, 2002] to as large as about 100 m [e.g., *Archuleta et al.*, 1982], with associated implications for stress drops for these events. These previous studies have calculated asperity size using an assumed value for slip, thus introducing a certain amount of circularity into the arguments.

[14] We exploit results from creep modeling on the Hayward fault [*Malservisi*, 2002] to improve the size estimates of asperities. Under the assumption that repeating earthquakes represent the repeated rupture of the same small asperity, and that the slip from these earthquakes is equivalent to the total slip on surrounding creeping patches over a certain time interval, we can estimate an approximate asperity size.

[15] We have selected five different sites of repeating earthquakes from the catalog determined by *Waldhauser and Ellsworth* [2002]. The locations of these clusters of events are shown in Figure 2. With the exception of cluster C, all are tight clusters. Cluster C potentially could be composed of more than one set of repeating earthquakes and thus might represent more than one asperity. In all cases the clusters we have chosen for this analysis are isolated from other non-repeating earthquakes.

Table 1. Results of Asperity Size Study

Asperity Group	Number of Earthquakes	Sum Mo (N-m)	Total Slip(m) Model	Asperity Size (m^2) Model
A	3	1.1×10^{11}	6.1×10^{-2}	6×10^1
B	8	9.2×10^{10}	5.4×10^{-2}	6×10^1
C	7	1.2×10^{13}	5.6×10^{-2}	7×10^3
D	11	3.4×10^{10}	5.6×10^{-2}	2×10^1
E	7	7.8×10^{10}	4.9×10^{-2}	5×10^1

Dataset spans 15 years. Locations of groups A through E are shown in Figure 2 See text for details.

[16] We have rearranged the standard seismic moment formula to solve for asperity size:

$$A = M_0 / (\mu * D) \quad (3)$$

where M_0 is the seismic moment (N-m), D is the slip (m), and μ is the shear modulus (30 GPa) for each asperity. We summed the seismic moments (determined using the above relations) for all recurrent earthquakes within each cluster. The total slip was simply the creep value for the corresponding element [using model KT3, *Malservisi, 2002*] over the 15-year time interval.

[17] Table 1 shows the results for the five different asperity sites. For A, B, D and E the calculated asperity size ranged from 20 to 60 m² (confirming the results of *Abercrombie [1995]*). For all groups, the asperity size increases with earthquake magnitude, following standard assumptions of earthquake mechanics. For group C, the calculated asperity size is larger. Group C is composed of larger earthquakes with several in the $M_1 > 2.5$ range. As a result the characteristic length scale for the asperity is ~ 100 m. With this length scale the relative locations of all of the events fall within that length, but the cluster could be divided into up to three separate sub-clusters separated by as much as 30 meters. If so, the resulting asperities for each sub-cluster would be smaller in size. If, rather than using the creep model slip value, we assign a slip value based on relations between moment and slip, we find that the average asperity sizes are an order of magnitude or more greater. This is because the slip values derived from earthquake relations are smaller than those derived from our creep models, leading to a larger area to accomplish the same seismic moment. Because of the wide range of values used in the scaling relationships, we tested several different values of stress drop to explore the effect of changes in this value on our results. Looking at Group E, for example, the asperity size can range from ~ 100 m² (using a stress drop of 0.01 MPa) to ~ 0.1 m² (using a stress drop of 10 MPa). For our preferred results (Table 1), we assumed a stress drop of ~ 0.8 MPa, based on the best-fit to *Abercrombie's [1995]* microseismic data (Figure 3). Although asperity sizes vary as a function of stress drop, the results confirm that the areas remain small, on a scale unlikely to be imaged by active seismic surveys. This further emphasizes the utility of including other information such as creep models to help "image" these small locking patches on faults.

4. Conclusions

[18] Along the Hayward Fault in the Eastern San Francisco Bay, the combination of precise relative locations for seismicity and geodynamic models of fault creep allows us to place robust constraints on the energy budget and asperity character of the fault zone. In particular we have shown that the microseismicity associated with fault creep releases an insignificant amount of the seismic moment on the fault, compared with both the moment released through aseismic creep and the moment deficit that is released during the rare large earthquakes on the Hayward fault. On areas of the fault that are relatively freely creeping there are clusters of earthquakes that appear to repeatedly rupture the same fault patch or asperity. By considering that rates of fault creep determined from our numerical models represent the inter-seismic slip in the region of these asperities, we can place

estimates on the area of the asperities associated with each cluster of repeated earthquakes. We find that for many of the clusters of repeating earthquakes, the characteristic area for the inferred asperities is approximately 100 m² or less.

[19] **Acknowledgments.** The authors would like to thank Bob Simpson and an anonymous reviewer for a careful reading of this manuscript and providing helpful comments. Further, we thank Felix Waldhauser for providing the microseismicity dataset. This research was supported by an NSF Graduate Research Fellowship to CRG and NSF Grant Numbers EAR 0003396 and EAR 0207520.

References

- Abercrombie, R., Earthquake source scaling relationships from -1 to 5 M_L using seismograms recorded at 2.5-km depth, *J. Geophys. Res.*, *100*(B12), 24,015–24,036, 1995.
- Aki, K., Scaling law of seismic spectrum, *Bull. Seismol. Soc. Am.*, *72*, 1217–1231, 1967.
- Aki, K., Magnitude-frequency relation for small earthquakes: A clue to the origin of f_{max} of large earthquakes, *J. Geophys. Res.*, *92*, 1349–1355, 1987.
- Amelung, F., and G. King, Earthquake scaling laws for creeping and non-creeping faults, *Geophys. Res. Lett.*, *24*(5), 507–510, 1997.
- Archuleta, R. J., E. Cranswick, C. Mueller, and P. Spudich, Source parameters of the 1980 Mammoth Lakes, California, earthquake sequence, *J. Geophys. Res.*, *87*, 4595–4607, 1982.
- Båth, M., Some properties of earthquake-frequency distributions, *Tectonophysics*, *51*(3–4), T63–T69, 1978.
- Bürgmann, R., D. Schmidt, R. M. Nadeau, M. d'Alessio, E. Fielding, D. Manaker, T. V. McEvilly, and M. H. Murray, Earthquake potential along the northern Hayward fault, California, *Science*, *289*, 1178–1181, 2000.
- Galehouse, J., Theodolite measurements of creep rates on San Francisco Bay region faults, *U.S. Geol. Surv. Open-File Rep.*, *92*(258), 256–261, 1992.
- Jennings, C. W., Fault activity map of California and adjacent areas, *Geologic Map*, 6, Department of Conservation Division of Mines and Geology, 1994.
- Johnson, L. R., and R. M. Nadeau, Asperity Model of an Earthquake: Static Problem, *Bull. Seism. Soc. Am.*, *92*(2), 672–686, 2002.
- Kanamori, H., J. Mori, E. Hauksson, T. H. Heaton, L. K. Hutton, and L. M. Jones, Determination of earthquake energy release and M_L using TERRASCOPE, *Bull. Seism. Soc. Am.*, *83*(2), 330–346, 1993.
- Lienkaemper, J., and J. Galehouse, New evidence doubles the seismic potential of the Hayward fault, *Seismol. Res. Lett.*, *69*(6), 519–523, 1998.
- Lienkaemper, J., G. Borchart, and M. Lisowski, Historic creep rate and potential for seismic slip along the Hayward fault, California, *J. Geophys. Res.*, *96*(B11), 18,261–18,283, 1991.
- Malservisi, R., Numerical Models of the dynamics of lithospheric deformation at complex plate boundaries, Ph.D. Thesis, The Pennsylvania State University, University Park, USA, pp. 125, 2002.
- Malservisi, R., C. Gans, and K. P. Furlong, Numerical modeling of strike-slip creeping faults and implications for the Hayward fault, California, *Tectonophysics*, *361*(1–2), 121–137, 2003.
- Nadeau, R. M., and L. R. Johnson, Seismological studies at Parkfield VI: Moment release rates and estimates of source parameters for small repeating earthquakes, *Bull. Seism. Soc. Am.*, *88*(3), 790–814, 1998.
- Rubin, A. M., D. Gillard, and J.-L. Got, Streaks of microearthquakes along creeping faults, *Nature*, *400*, 635–641, 1999.
- Scholz, C. H., The mechanics of earthquakes and faulting, Cambridge University Press, New York, 1990.
- Simpson, R. W., J. J. Lienkaemper, and J. S. Galehouse, Variations in creep rates along the Hayward fault, California, interpreted as changes in depth of creep, *Geophys. Res. Lett.*, *28*(11), 2269–2272, 2001.
- Smith, S. W., and M. Wyss, Displacement on the San Andreas fault subsequent to the 1966 Parkfield earthquake, *Bull. Seism. Soc. Am.*, *58*(6), 1955–1973, 1968.
- Thatcher, W., and T. Hanks, Source parameters of southern California earthquakes, *J. Geophys. Res.*, *78*, 8547–8576, 1973.
- Waldhauser, W., and F. Ellsworth, Fault structure and mechanics of the Hayward Fault, California, from double-difference earthquake locations, *J. Geophys. Res.*, *107*(B3), doi:10.1029/2000JB000084, 2002.

C. R. Gans and K. P. Furlong, Geodynamics Research Group, Department of Geosciences, Pennsylvania State University, University Park, PA, USA. (cgans@geodyn.psu.edu)

R. Malservisi, Rosenstiel School of Marine and Atmospheric Science, University of Miami, Miami, FL, USA.